Articles

Spin Coupling through the N→Si Dative Bond in Penta- and Hexacoordinate Hydrido- and Fluorosilicon Complexes; Coupling through a Rapidly Dissociating−Recombining N→Si Bond

Inna Kalikhman,*[,†] Boris Gostevskii,[†,‡] Vijeyakumar Kingston,[†] Sonia Krivonos,[†] Dietmar Stalke,[§] Bernhard Walfort,[§] Thomas Kottke,[§] Nikolaus Kocher,[§] and Daniel Kost*[,†]

Department of Chemistry, Ben-Gurion University, Beer-Sheva 84105, Israel, A. E. Favorsky Irkutsk Institute of Chemistry, Russian Academy of Sciences, Siberian Branch, 664033 Irkutsk, Russia, and Institut für Anorganische Chemie, Universität Würzburg, am Hubland, D-97074 Würzburg, Germany

Received June 28, 2004

Penta- and hexacoordinate silicon complexes with spin $^1/_2$ nuclei (^{1}H and ^{19}F) directly attached to silicon have been prepared and used to study NMR spin−spin interactions across the N→Si dative bond. In both hydrido and fluoro complexes, two-bond coupling constants were found to drop sharply as the geminal bond angle deviated from 90°. Three-bond coupling constants showed a Karplus-type dependence upon the corresponding dihedral angles for both ^{1}H and ^{19}F complexes. Four-bond coupling constants $^4J(^{19}F-Si-N-C-^1H)$ across the dative bond were observed. The correlations can be used as tools for the interpolation of bond and dihedral angles from NMR data, in cases where crystal structures are unavailable. They also demonstrate that the N→Si dative bond in hypercoordinate silicon complexes behaves essentially in the manner expected from normal covalent bonds. Rapid dissociation and recombination of the N−Si dative bond was established in several pentacoordinate complexes; however, one-, two-, and three-bond coupling constants could nevertheless be measured across this rapidly dissociating bond.

Introduction

Hypercoordinate silicon compounds have attracted substantial interest in recent years and have been extensively reviewed.[1] Despite the wide attention, some aspects of hypercoordination in silicon compounds are not fully understood and deserve further investigation. These include the nature of the dative bond between donor atoms, normally oxygen or nitrogen, and silicon.[2] One structural aspect of the dative bond, which may reflect on its properties, is the spin−spin interaction between nuclei located on both sides of the bond.[3] The magnitude of the coupling constants across the dative bond, as well as its dependence on bond and dihedral angles, is a sensitive probe into the structure of silicon complexes in solution and the nature of the dative bond.

Ideally, one would like to probe the direct donor−acceptor interaction: i.e., the one-bond coupling constant between ^{29}Si and the donor nitrogen ^{15}N. This would directly reflect bonding properties of the dative bond and provide the desired insight. The presence of a measurable one-bond donor−acceptor coupling constant is definite evidence for the existence of coordination *in solution*.[4] However, the $^{15}N-^{29}Si$ coupling constant is exceedingly difficult to measure, due to the low relative

[†] Ben-Gurion University.
[‡] A. E. Favorskii Irkutsk Institute of Chemistry.
[§] Universität Würzburg.

(1) (a) Tandura, S. N.; Voronkov, M. G.; Alekseev, N. V. *Top. Curr. Chem.* **1986**, *131*, 99. (b) Kost, D.; Kalikhman, I. In *The Chemistry of Organic Silicon Compounds*; Rappoport, Z., Apeloig, Y., Eds.; Wiley: Chichester, U.K,, 1998; Vol. 2, Part 2, pp 1339−1445. (c) Lukevics, E.; Pudova, O. A. *Chem. Heterocycl. Compd. (Engl. Transl.)* **1996**, *32*, 1381. (d) Holmes, R. R. *Chem. Rev.* **1996**, *96*, 927. (e) Chuit, C.; Corriu, R. J. P.; Reyé, C. In *The Chemistry of Hypervalent Compounds*; Akiba, K.-Y., Ed.; Wiley-VCH: New York, 1999; pp 81−146. (f) Bassindale, A. R.; Taylor, P. G. In *The Chemistry of Organic Silicon Compounds*; Patai, S., Rappoport, Z., Eds.; Wiley: Chichester, U.K., 1989; Vol. 1, Part 1, pp 839−892. (g) Kira, M.; Zhang, L. C. In *The Chemistry of Hypervalent Compounds*; Akiba, K.-Y. Ed.; Wiley-VCH: New York, 1999; pp 147−198. (h) Brook, M. A. *Silicon in Organic, Organometallic, and Polymer Chemistry*; Wiley: New York; 2000; pp 97−114. (i) Verkade, J. G. *Coord. Chem. Rev.* **1994**, *137*, 233. (j) Tacke, R.; Pülm, M.; Wagner, B. *Adv. Organomet. Chem.* **1999**, *44*, 221. (k) Kost, D.; Kalikhman, I. *Adv. Organomet. Chem.* **2004**, *50*, 1.

(2) Kocher, N.; Henn, J.; Gostevskii, B.; Kost, D.; Kalikhman, I.; Engels, B.; Stalke, D. *J. Am. Chem. Soc.* **2004**, *126*, 5563.

(3) Ando, I.; Webb, G. A. *Theory of NMR Parameters*; Academic Press: London, 1983; p 83.

(4) (a) Pestunovich, V. A.; Shterenberg, B. Z.; Voronkov, M. G.; Magi, M. J.; Samoson, A. V. *Izv. Akad. Nauk SSSR, Ser. Khim.* **1982**, 1435. (b) Kupce, E.; Liepins, E.; Lapsina, A.; Urtane, I.; Zelcans, G.; Lukevics, E. *J. Organomet. Chem.* **1985**, *279*, 343. (c) Kupce, E.; Lukevics, E. *J. Organomet. Chem.* **1988**, *358*, 67 and references therein. (d) Nakash, M.; Goldvaser, M. *J. Am. Chem. Soc.* **2004**, *126*, 3436.

10.1021/om049530k CCC: $27.50
Publication on Web 09/15/2004

Table 1. Crystal Data and Experimental Parameters for the Crystal Structure Analyses of 1 and 2b,c

	1	2b	2c
empirical formula	$C_{15}H_{17}ClN_2OSi$	$C_{14}H_{31}ClN_4O_2Si$	$C_{14}H_{31}BrN_4O_2Si$
formula mass, g mol^{-1}	304.85	350.97	395.43
collection T, K	173(2)	100(2)	100(2)
λ(Mo Kα), Å	0.710 73	0.710 73	0.710 73
cryst syst	monoclinic	triclinic	triclinic
space group	$P2_1/c$	$P\bar{1}$	$P\bar{1}$
a, Å	7.4781(11)	8.8906 (4)	8.9320(5)
b, Å	16.8480 (15)	15.1374(7)	15.1189(8)
c, Å	12.3734(19)	15.6639(7)	15.7812(8)
α, deg	90	113.0730(10)	111.8950
β, deg	92.719(7)	93.8240(10)	94.3350(10)
γ, deg	90	96.6450(10)	96.3620(10)
V, Å^3	1557.2(4)	1911.86(15)	1949.37(18)
Z	4	4	4
ρ_{calcd}, Mg/m^3	1.300	1.219	1.347
F(000)	640	760	832
θ range, deg	3.30−24.99	1.42−28.33	1.40−26.38
no. of collected rflns	5100	38 006	41 397
no. of indep rflns	2730	8880	7959
R_{int}	0.0181	0.0196	0.0208
no. of rflns used	2730	8880	7959
no. of params	187	425	425
GOF	1.021	1.033	1.037
R1,[a] wR2[b] ($I > 2\sigma(I)$)	0.0343, 0.0703	0.0338, 0.0895	0.0313, 0.0904
R1,[a] wR2[b] (all data)	0.0524, 0.0769	0.0362, 0.0911	0.0332, 0.0916
max, min res electron dens (e Å^{-3})	0.289, −0.218	+0.703, −0.219	+0.584, −0.469

[a] $R1 = \sum||F_o| - |F_c||/\sum|F_o|$. [b] $wR2 = \{\sum[w(F_o^2 - F_c^2)^2]/\sum[w(F_o^2)^2]\}^{1/2}$.

abundances of the spin $^1/_2$ nuclei in natural nitrogen and silicon compounds.[4]

Measurement of spin interactions between ^{1}H or ^{19}F attached directly to silicon and other nuclei on the other side of the dative bond offers a more practical opportunity to investigate the dative bond. We now report on the direct measurement of coupling constants between ^{1}H or ^{19}F (in hydrido and fluoro complexes, respectively) and ^{15}N, ^{13}C, or ^{1}H nuclei situated on the opposite end of the N→Si bond. Crystal structures have been analyzed for several of these hydrido and fluoro penta- and hexacoordinate silicon complexes, allowing a study of the correlation between coupling constants and molecular geometries.[5] In addition, a case of observation of spin−spin coupling across the N→Si dative bond *while this bond is rapidly dissociating and recombining* is described.

Results and Discussion

1. Synthesis and Structure. All of the complexes described here are derivatives of hydrazides and have been prepared in high yields by trans-silylation of *O*-(trimethylsilyl)-*N*-(dimethylamino)acylimidates ("TMS-hydrazides") and di-, tri-, or tetrahalosilanes, using a method developed and described previously.[6] In this way compounds **1**−**4** were prepared, having in common a spin $^1/_2$ ligand (hydrido or fluoro) attached to silicon. This feature allows facile measurement of coupling constants between the H or F ligands and silicon, nitrogen, or *N*-methyl carbon.

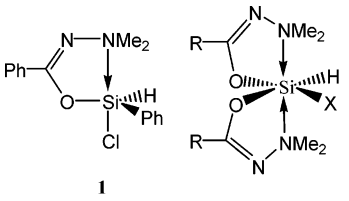

1

2a, R = Me, X = Cl
2b, R = *t*-Bu, X = Cl
2c, R = *t*-Bu, X = Br
2d, R = Ph, X = Cl
2e, R = CF_3, X = Cl

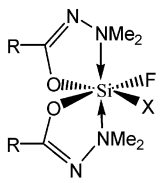

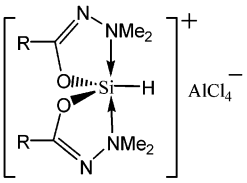

3, R = CF_3, X = Ph
4a, R = Ph, X = F
4b, R = CF_3, X = F
4c, R = NMe_2, X = F

5a, R = Me
5b, R = *t*-Bu

Interestingly, the trans-silylation procedure leads to a variety of different complex types: neutral penta-[6b] and hexacoordinate[6a] complexes, as well as cationic pentacoordinate complexes.[7]

A number of these compounds were crystallized, and their crystal structures were analyzed. The structures of **2e**,[5a] **3**,[5a] **4a**,[8] and **4b**[5a] were reported previously. The crystallographic analyses for compounds **1** and **2b**,**c** have now been obtained and are summarized in Table 1 and depicted in Figures 1−3. Selected geometrical data are given in Table 2.

(5) For preliminary results see: (a) Kalikhman, I.; Krivonos, S.; Stalke, D.; Kottke, T.; Kost, D. *Organometallics* **1997**, *16*, 3255. (b) Kalikhman, I.; Krivonos, S.; Kottke, T.; Stalke, D.; Kost, D. In *Organosilicon Chemistry IV*; Auner, N., Weis, J., Eds.; Wiley-VCH: Weinheim, Germany, 2000; pp 494−499.

(6) (a) Kost, D.; Kalikhman, I.; Raban, M. *J. Am. Chem. Soc.* **1995**, *117*, 11512. (b) Kalikhman, I.; Krivonos, S.; Ellern, A.; Kost, D. *Organometallics* **1996**, *15*, 5073.

(7) Kost, D.; Kingston, V.; Gostevskii, B.; Ellern, A.; Stalke, D.; Walfort, B.; Kalikhman, I. *Organometallics* **2002**, *21*, 2293.

(8) Kalikhman, I.; Gostevskii, B.; Girshberg, O.; Sivaramakrishna, A.; Kocher, N.; Stalke, D.; Kost, D. *J. Organomet. Chem.* **2003**, *686*, 202.

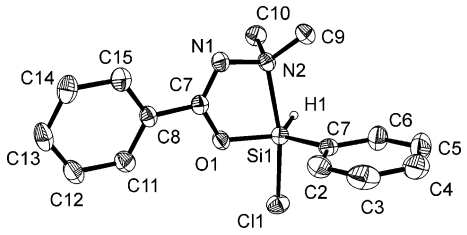

Figure 1. Crystallographic molecular structure of **1**, presented at the 50% probability level. Hydrogen atoms, except the hydrido hydrogen, have been omitted for clarity.

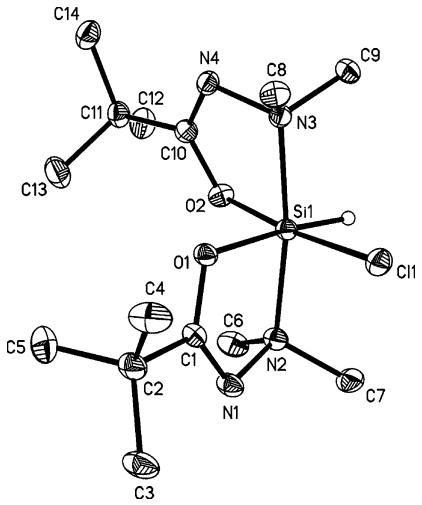

Figure 2. Crystallographic molecular structure of **2b**, presented at the 50% probability level. Hydrogen atoms, except the hydrido hydrogen, have been omitted for clarity.

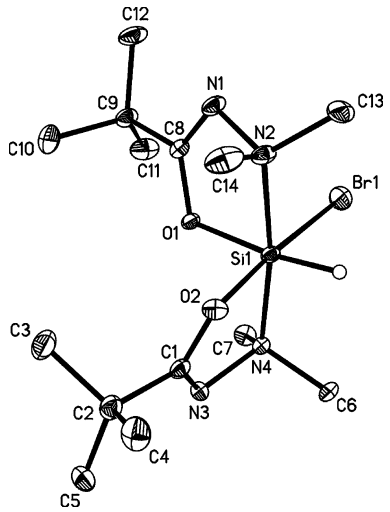

Figure 3. Crystallographic molecular structure of **2c**, presented at the 50% probability level. Hydrogen atoms, except the hydrido hydrogen, have been omitted for clarity.

2. Hydrido Complexes. (a) Two-Bond Coupling. The natural-abundance ^{15}N NMR spectra, fully ^{1}H-coupled, of **2a**−**e** and **1** have been measured, and the ^{15}N chemical shifts and $^{2}J(^{1}H-Si-^{15}N)$ coupling constants are listed in Table 3. The two diastereotopic nitrogen atoms adjacent to silicon in **2d**,**e** give rise to two resonances and two coupling constants in toluene-d_8 solution, in which chelate exchange is slow relative to the NMR time scale. However, in other solvents ($CDCl_3$ and nitrobenzene-d_5) exchange is rapid, and hence, only one average coupling constant (and chemical shift) is observed (Table 3).[6a] A fully ^{1}H-coupled ^{15}N NMR spectrum, that of **2e** (toluene-d_8), is displayed in Figure 4, showing two doublets for the NMe_2 groups, with $^{2}J(^{1}H-Si-^{15}N)$ coupling constants of 10.2 and 12.0 Hz. (The $^{2}J(^{15}N-C-^{1}H_3)$ values are negligibly small and are not observed.) It is thus demonstrated that spin−spin interactions are transmitted through the dative N→Si bond and can be observed and measured.

A dramatic dependence of the geminal $^{1}H-^{15}N$ coupling constant on the corresponding H−Si−N bond angle is found and is depicted in Figure 5: the interaction is maximal at a 90° bond angle, and it drops rapidly upon increasing or decreasing the angle. In Figure 5 the geminal coupling constant is plotted against the *deviation* of the bond angle from 90°, in either direction. When the two points taken from the literature for compounds $N(SiH_3)_3$ (**6**)[9] and **7**[4b] are included, in which

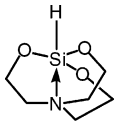

7

the bond angles are 109 and 180°, respectively, an exponential drop of coupling constant vs angle is found, similar in shape to coupling constants in a CH_2 group.[10] The greatest sensitivity of spin−spin interactions to-

Table 2. Selected Crystallographic Bond Lengths and Angles for 1 and 2b,c

	1	2b[a]		2c[a]	
		Bond Distances (Å)			
Si−O	1.6948(14)	1.7490(8)	1.7535(9)	1.7401(13)	1.7470(14)
		1.7757(9)	1.7628(9)	1.7649(15)	1.7536(16)
Si−N	2.1582(17)	1.9825(10)	1.9806(11)	1.9790(17)	1.9775(18)
		1.9583(10)	2.0019(11)	1.9940(16)	2.0073(19)
Si−H	1.373(19)	1.37(2)	1.40(2)	1.34(2)	1.44(3)
Si−Cl(Br)	2.1602(8)	2.2454(4)	2.2327(5)	2.4503(6)	2.4374(6)
		Bond Angles (deg)			
N−Si−N		171,20(4)	171.35(5)	171.51(7)	171.73(8)
N− Si−Cl	167.80(6)	92.68(3)	91.38(3)	92.32(6)	91.29(5)
		90.86(3)	93.51(4)	90.61(5)	92.93(6)
O−Si−Cl	91.33(5)	89.59(3)	88.70(3)	88.78 (5)	87.88(5)
		173.27(3)	174.53(3)	173.41(5)	174.87(6)

[a] Bond lengths and angles are reported for two molecules in the unit cell.

Table 3. ^{15}N NMR Chemical Shifts and Geminal $^{2}J(^{15}N-Si-^{1}H)$ Coupling Constants for Complexes 1 and 2 in Different Solvents

compd	solvent	$\delta(^{15}N{=}C)$ (ppm)	$\delta(^{15}NMe_2)$ (ppm)	$^{2}J(^{15}N-Si-^{1}H)$ (Hz)
1	$CDCl_3$	255.4	66.8	10.8
2a	$CDCl_3$	237.5	65.6	11.4
2a	NO_2Ph-d_5	239.1	65.2	11.7
2b	$CDCl_3$	232.7	60.6	10.7
2d	toluene-d_8	240.0	67.8	10.3
		239.3	64.4	12.8
2d	NO_2Ph	239.3	65.8	11.7
2e	toluene-d_8	247.3	68.4	10.2
		249.2	65.7	12.0
5a	$CDCl_3$	249.1	66.7	12.9
5b	$CDCl_3$	254.9	67.2	13.7

(9) Anderson, D. W. N.; Benthan, J. E.; Rankin, D. W. H. *J. Chem. Soc., Dalton Trans.* **1973**, 1215.

(10) Silverstein, R. M.; Bassler, G. C.; Morrill, T. C. *Spectrometric Identification of Organic Compounds*, 5th ed.; Wiley: New York, 1991; p 197.

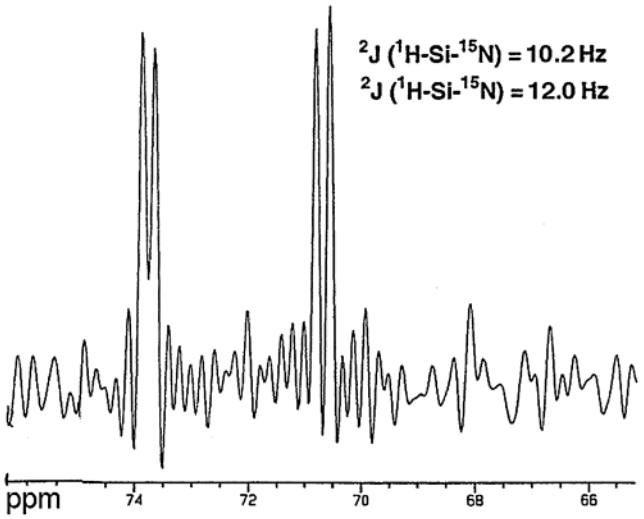

Figure 4. Natural-abundance, fully ^{1}H-coupled ^{15}N NMR spectrum of **2e** in toluene-d_8 solution at 300 K. The *N*-methyl region is shown.

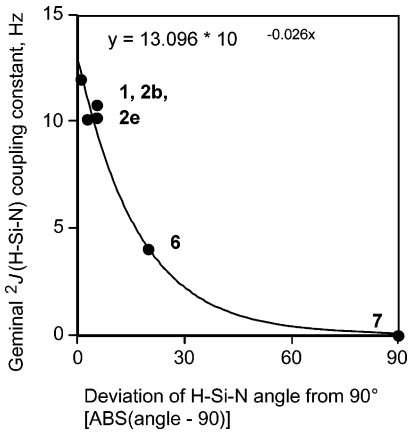

Figure 5. Geminal (^{1}H−Si−^{15}N) coupling constants for **1** and **2b**,**e** (this work), and **6**,[9] and **7**[4b] plotted against the *deviation* of the H−Si−N angle from 90°. The exponential best fit function is shown.

ward changes in bond angle is near 90°, and hence, this correlation can be useful as a tool for assessing H−Si−N bond angles in other silicon complexes *in solution* and, in particular, small changes near 90°.

A second important effect on the magnitude of the geminal coupling constant is the effect of N→Si dative-bond length. This is best demonstrated by comparison of the geminal coupling constants of **2b** and **5b** (Table 3): the geminal coupling constant ^2J(^{1}H−Si−^{15}N) = 13.7 Hz in **5b** is the largest observed in this series of compounds. This must be due to the shorter N−Si distance in **5b** relative to those in the neutral hexacoordinate complexes **2**, and specifically **2b**. The evidence for a shorter N−Si distance in the ionic vs the neutral complex is indirect, from a comparison of two analogous

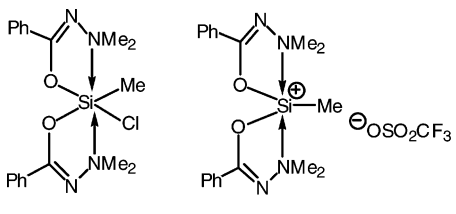

Table 4. Crystallographic (H−Si−N−C) Dihedral Angles and the Corresponding Vicinal Coupling Constants from ^{1}H-Coupled ^{13}C NMR Spectra

compd	dihedral angle (deg)	^3J(^{1}HSiN^{13}C) (Hz)	solvent	T[a] (K)
1	28.3	1.7	$CDCl_3$	243
	97.5	0		
2b	136.0 (130.5)	0.7	toluene-d_8	265
	9.9 (−5.4)	2.6		
	79.3 (−83.4)	0		
	−44.8 (40.7)	0.4		
2c	−129.5 (−134.4)	0.7	toluene-d_8	185[b]
	−3.9 (−7.2)	3		
	36.4 (36.5)	1		
	−84.8 (−88.1)	0		
2e	157.4	2.4	CD_2Cl_2	243
	31.9	1.1		
	49.3	0.4		
	−76.1	0		
5a		2.1	CD_2Cl_2	300
		0		
5e		2.0	CD_2Cl_2	300
		0		

[a] Solutions were cooled to eliminate exchange-broadening phenomena. [b] At 185 K exchange broadening of signals is still significant, and hence the uncertainty in coupling constants may be as high as 50%.

complexes, **8**[11] and **9**,[7] for which crystal structures are available: the corresponding N−Si bond lengths in **8** and **9** are 2.015(7) and 1.9665(17) Å, respectively. A similar trend in geminal ^{15}N−Si−^{1}H coupling constants has been observed for the pair **2a** and **5a** (Table 3), though to a smaller extent.

(b) Three-Bond Coupling: Karplus Correlation. The hydrido complexes also permit measurement of vicinal ^3J(^{1}H−Si−N−^{13}C) coupling constants, between the hydrido proton and the *N*-methyl carbon nuclei. To this end, the ^{1}H-coupled ^{13}C NMR spectra were measured, and the multiplets due to the four (nonequivalent) *N*-methyl carbons were carefully analyzed. Each methyl carbon resonance is split twice, by its own protons and by the neighboring *N*-methyl protons, into a quartet of quartets. In addition, some of these quartets are further split by the Si−*H* proton. These three-bond couplings are listed in Table 4. Each of the vicinal coupling constants can be matched with a corresponding crystallographic dihedral angle. Thus, for example, in compound **1** there are two H−Si−N−C dihedral angles, 97.5 and 28.3°, and two corresponding observed vicinal coupling constants, 0 and 1.7 Hz. We assign the former dihedral angle to the negligible coupling constant and the remaining angle to the significant coupling constant. This is done for four *N*-methyl carbon signals in the hexacoordinate complexes **2b**,**c**,**e**, as well as for two signals in the pentacoordinate **1**. The resulting vicinal coupling constants have been plotted against the most reasonable (best matched) corresponding crystallographic dihedral angles, as depicted in Figure 6.

It is obvious from Figure 6 that the vicinal coupling constants across the dative bond follow a Karplus-type correlation with the corresponding dihedral angles. The best-fit second-order polynomial equation connecting the experimental points is shown in Figure 6.[12] The observation of this correlation is evidence for the "normal"

(11) Mozzhukhin, A. O.; Antipin, M. Yu.; Struchkov, Yu. T.; Gostevskii, B. A.; Kalikhman, I. D.; Pestunovich, V. A.; Voronkov, M. G. *Metalloorg. Khim.* **1992,** *5*, 658; *Chem. Abstr.* **1992**, *117*, 234095w.

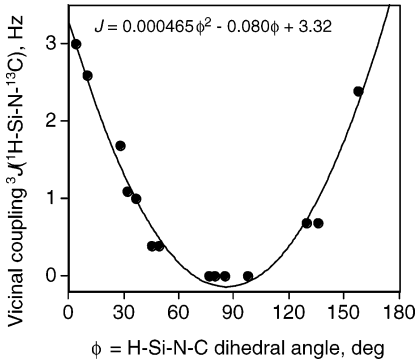

Figure 6. Plot of vicinal (^{1}H−Si−N−^{13}C) coupling constants for **1**, **2b**,**c**,**e** as a function of the corresponding crystallographic dihedral angles.

behavior of the N→Si dative bond, as is found for vicinal coupling in H−C−C−H arrangements. Interestingly, both penta- and hexacoordinate compounds fit the same Karplus correlation, within experimental error. Figure 6 and the associated quadratic equation can serve as a tool for assessing dihedral angles for hexa- and pentacoordinate hydridosilicon complexes in solution, for which crystallographic molecular structures are not available.

An apparently similar trend in vicinal coupling constants has been observed also in the pentacoordinate cationic silicon complexes **5a**,**b**: three-bond coupling is observed between the hydrido proton and *one* of the two *N*-methyl carbon nuclei (see Table 4), presumably the methyl group which forms a near-zero dihedral angle with the hydrido proton. This specific spin−spin interaction to only one of the two *N*-methyl groups has been confirmed by a COLOC (long-range C−H correlation) experiment, showing no interaction with one of the methyl groups.

(c) Stereodynamics of 1. The neutral pentacoordinate **1** deserves further attention: at temperatures below room temperature (263 K), the two *N*-methyl groups are fully resolved, and the individual vicinal coupling constants can be measured (Table 4). As the temperature of the solution is raised, coalescence of the signals arising from the diastereotopic *N*-methyl groups is observed (T_c = 310 K, ΔG^* = 14.6 kcal mol^{-1}). The observation of two resonances for the *N*-methyl groups at low temperature is evidence for the N−Si coordination. The coalescence process proves that exchange takes place in **1** which renders these diastereotopic *N*-methyl groups homotopic. However, there are two plausible mechanisms which may render the methyl groups equivalent: either dissociation of the N→Si dative bond, followed by rotation about the N−N bond and recombination, or inversion of configuration at the chiral silicon center, presumably by pseudorotation. The two alternative exchange mechanisms are indistinguishable on the basis of the available NMR data.

To assign the correct mechanism complex **10**, an analogue of **1** in which a chiral carbon center (CH(Ph)Me) has been incorporated was prepared.[6b] The variable-temperature ^{1}H NMR spectra of **10** (shown in

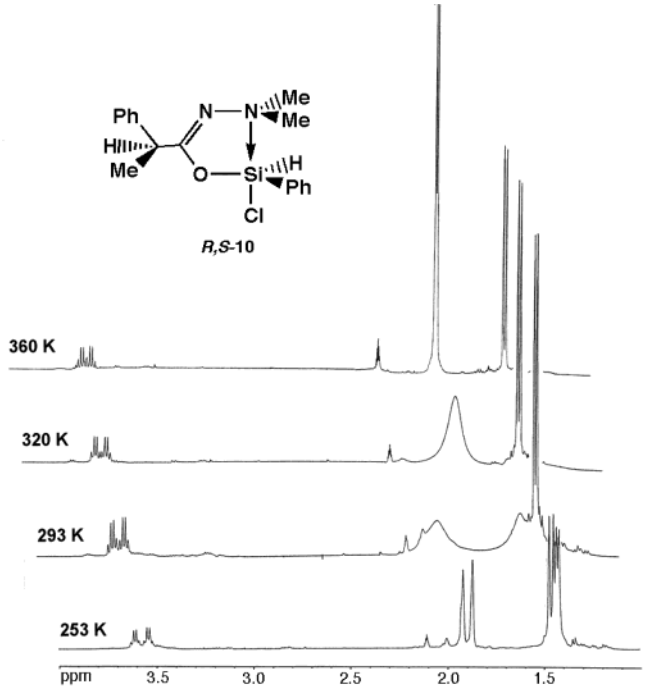

Figure 7. ^{1}H NMR spectra of **10** in toluene-d_8 solution at various temperatures.

Figure 7) provide the mechanistic assignment:[5b] at low temperature, two sets of signals are observed corresponding to two diastereomers (due to the presence of two chiral centers, at silicon and at carbon). Thus *four* *N*-methyl singlets are found, two for each diastereomer. When the temperature is increased, the latter gradually broaden, coalesce, and finally (at 360 K) give rise to two sharp singlets, as a result of rapid *N*-methyl exchange within each diastereomer, relative to the NMR time scale. However, throughout this process no exchange *between* diastereomers is observed, as evident from the presence at all temperatures of *two* CCH_3 and two C*H* signals. This means that at this temperature range the diastereomers do not exchange and, hence, that no inversion of configuration takes place at either silicon or carbon. The observed exchange of *N*-methyl groups must therefore result from the alternative process, rapid dissociation of the N→Si coordination bond, associated with loss of identity of each *N*-methyl group (eq 1).

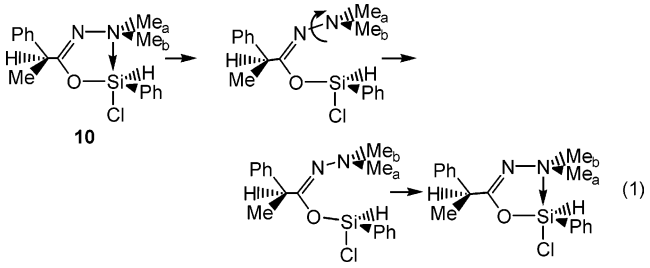

(d) Coupling through a Rapidly Dissociating N→Si Bond. The assignment of the exchange process in **10**, and by analogy also in **1**, to N−Si dissociation−recombination leads to another interesting observation: the natural-abundance ^{15}N NMR spectrum of **1** at ambient temperature features a doublet, due to geminal coupling by the hydrido proton. However, this coupling is observed despite the fact that at this

(12) Interestingly, a parabola provided a significantly better fit to the data than various periodic functions used previously as Karplus functions: (a) Karplus M. *J. Chem. Phys.* **1959**, *30*, 11. (b) Günter, H. *NMR Spectroscopy*; Wiley: Chichester, U.K., 1994; p 115.

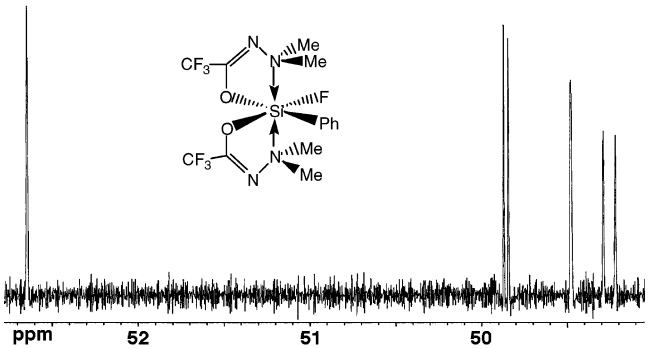

Figure 8. $^{13}C\{^1H\}$ NMR spectrum of **3** (N−CH_3 region) in CD_2Cl_2 solution at 253 K, showing different vicinal $^{19}F-^{13}C$ coupling constants for each methyl group.

temperature the evidence (mentioned above) indicates rapid dissociation−recombination of the N→Si bond. It is thus evident that rapid dissociation does not result in spin inversion of the nitrogen nucleus and, hence, in preservation of the spin−spin interaction.

3. Fluoro Complexes. (a) Two-Bond Coupling. The crystal structures of three fluoro complexes, **3**,[5a] **4a**,[8] and **4b**,[5a] have been analyzed and reported. The ^{15}N NMR spectra for two of these complexes, **3** and **4b**, have been measured and show two-bond coupling constants between the fluoro ligands and the donor nitrogen atoms extending across the N→Si dative bond. As in the hydrido case discussed above, the geminal F−Si−N interactions are highly sensitive to the bond angle. Thus, the two F−Si−N bond angles in **3**, 91.23 and 96.85°, correspond to geminal coupling constants $^2J(^{19}F-Si-^{15}N)$ of 9.0 and 4.5 Hz, respectively: i.e., a change of less than 5° in bond angle generates a 50% decrease in coupling constant!

The bond-angle effect on spin−spin interaction cannot be completely isolated from the effect of dative-bond length. Thus, in the difluoro complex **4b** the N→Si distances are significantly shorter than in **3** (1.96 and 2.02 Å, respectively). As a result, the geminal $^{19}F-^{15}N$ interaction is significantly greater in **4b** than in **3**. This is evident from the average coupling constant observed in **4b**, 12.2 Hz, which is greater than both of the coupling constants measured in **3**, although the corresponding F−Si−N bond angles in the crystal are slightly smaller in **4b** (91.12 and 95.39°) than in **3**. The observation of only one average two-bond coupling constant in **4b**, in contrast to **3**, is a result of rapid exchange of the fluoro ligands in solution of **4b**, relative to the NMR time scale.

(b) Three-Bond Coupling. The $^{13}C\{^1H\}$ NMR spectrum of **3** (*N*-methyl region) is shown in Figure 8. No apparent exchange processes take place relative to the NMR time scale at this temperature, and all four diastereotopic *N*-methyl groups give rise to corresponding signals in the spectrum. These signals are each split by coupling to the ^{19}F nucleus of the fluoro ligand. The crystallographic F−Si−N−C dihedral angles (ϕ) and the corresponding three-bond $^3J(^{19}F-Si-N-^{13}C)$ coupling constants are listed in Table 5. From these data a Karplus-type correlation has been plotted (Figure 9), and the least-squares best-fit second-order polynomial has been calculated and drawn. As in the hydrido complexes, Figure 9 suggests that in the fluoro complexes a Karplus type correlation controls the vicinal coupling constants across the dative bond.

Table 5. Crystallographic (F−Si−N−C) Dihedral Angles and the Corresponding Three-Bond Coupling Constants[a]

complex	∠F−SiN−C (deg)	NMe[b]	δ (ppm (multiplicity))	$^3J(^{19}F-^{13}C)$ (Hz)	interpolated $^3J(^{19}F-^{13}C)$ (Hz)
3[c]	138.9	a	49.5 (d)	0.8	
	14.6	b	49.3 (d)	9.1	
	40.4	a′	49.9 (d)	3.4	
	−83.9	b′	52.7 (s)	0	
4a	141.5	a		1.0	1.2
	17.9	b		5.4	8.1
	49.9	a′			2.6
	−79.7	b′			0.1
4b	143.1	a	50.1 (t)	1.4	1.5
	20.0	b	50.3 (t)	5.4	7.7
	49.3	a′			2.7
	−73.8	b′			0.2
4c	-	a, a′	51.8 (t)	1.4	
	-	b, b′	52.0 (t)	5.3	

[a] Due to rapid ligand exchange in **4a**−**c**, only two average coupling constants are measured. The four individual constants in **4a**,**b** were obtained by interpolation (Figure 9). [b] The assignment of geminal *N*-methyl pairs (a−b and a′−b′) is based on ^1H one- and two-dimensional NOE experiments, followed by $^1H-^{13}C$ 2D correlation spectra. [c] ^{13}C NMR for **3** in CD_2Cl_2 solution at 243 K and for **4a**−**c** in $CDCl_3$ solution at 300 K.

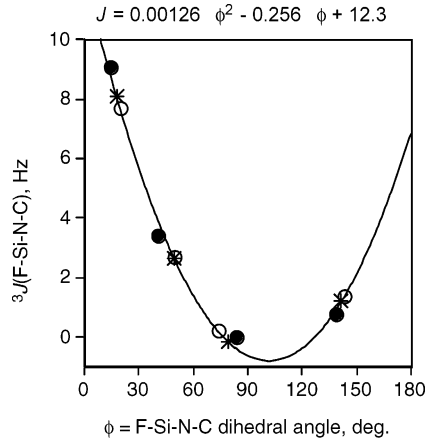

Figure 9. Vicinal ($^{19}F-Si-N-^{13}C$) coupling constants for **3** (●), **4a** (*), and **4b** (○). The second-order polynomial equation was drawn to fit the data for **3**; the points for **4a**,**b** were calculated from the crystallographic angles using the equation.

The ^{13}C NMR spectra for the other three fluoro complexes, **4a**−**c**, are complicated by rapid ligand-site exchange: the vicinal interactions between the fluoro and *N*-methyl carbon nuclei are averaged through rapid exchange of the fluoro ligands, giving rise to triplets, with only two unique $^3J(^{19}F-Si-N-^{13}C)$ coupling constants (Table 5). In the absence of individual coupling constants, the average values cannot be placed directly on the Karplus correlation. However, the crystallographic dihedral angles have been used with the parabola equation to interpolate the four individual coupling constants. These are shown in Figure 9 and listed in Table 5. The average ^3J value for each pair of interpolated coupling constants for nongeminal *N*-methyl groups (a with b′ and b with a′) is in excellent agreement with the two measured $^3J(^{19}F-Si-N-^{13}C)$

Table 6. Coupling Constants $^4J(^{19}F-Si-N-C-^1H)$ from ^1H NMR of NMe Groups

compd	δ (ppm (multiplicity))	$^4J(^{19}FSiN^1H)$ (Hz)	solvent	T (K)
3	2.25 (s)	0	CD_2Cl_2	253
	2.65 (br s)	<0.6		
	2.68 (d)	0.8		
	3.17 (d)	2.2		
4a	3.02 (t)	1.5	$CDCl_3$	300
	3.20 (t)	0.7		
4b	2.87 (t)	1.6	$CDCl_3$	300
	2.94 (t)	0.7		
4c	2.77 (t)	1.4	$CDCl_3$	300
	2.84 (br s)	0		

coupling constants for each complex, evidence for the general application of the Karplus correlation.

The correlation equation may also be used in the opposite sense, for the interpolation of dihedral angles from available ^3J coupling constants. This may be useful for fluoro complexes for which crystal structures are not available.

(c) Four-Bond Coupling. Four-bond coupling constants ($^{19}F-Si-N-C-^1H$) have also been measured, in the ^1H NMR spectra of mono- and difluoro complexes **3** and **4** (Table 6). The observed four-bond coupling constants are different for the diastereotopic *N*-methyl groups in each compound, evidence that they also, like the three-bond couplings, are stereochemically selective. They are also complicated by rapid exchange and averaging of signals. It may be concluded that the spin−spin interactions are carried through the dative bond over two, three, and even four bonds, as in other compounds with ordinary covalent bonding. In that sense the dative bond behaves in full analogy with a regular covalent bond.

Experimental Section

The reactions were carried out under dry argon using Schlenk techniques. Solvents were dried and purified by standard methods. NMR spectra were recorded on a Bruker Avance DMX-500 spectrometer operating at 500.13, 125.76, 50.68, and 99.36 MHz, respectively, for ^1H, ^{13}C, ^{15}N, and ^{29}Si spectra. Spectra are reported in δ (ppm) relative to TMS, as determined from standard residual solvent proton (or carbon) signals for ^1H and ^{13}C and directly from TMS for ^{29}Si, and relative to external $^{15}NH_4Cl$ for ^{15}N. All the geminal N−Si−H coupling constants reported were verified by broad-band ^1H-decoupled ^{15}N spectra, ($^{15}N\{^1H\}$), and all vicinal H−Si−N−C coupling constants were verified by long-range C−H COLOC correlation spectra. Natural-abundance ^{15}N NMR spectra were measured in 10 mm NMR tubes with concentrated solutions (ca. 30%), applying 30° pulses (12 μs) and 11−15 s delay between pulses, for 24 h. $^2J(^{15}N-^1H)$ values are estimated to be accurate to ±0.4 Hz. Melting points were measured in sealed capillaries using a Buchi melting point instrument and are uncorrected. Elemental analyses were performed by Mikroanalytisches Laboratorium Beller, Göttingen, Germany.

The following compounds were reported previously: **2a**,[6a] **2d**,[6a] **2e**,[6a] **3**,[5a] **4a**,[8] and **4b**.[5a]

[*N*-(dimethylamino)benzimidato-*N,O*]chlorohydridophenylsilicon(IV) (1). To a solution of 0.589 g (3.33 mmol) of $PhHSiCl_2$ in 5 mL of chloroform was added 0.697 g (2.93 mmol) of *N*-(dimethylamino)-*O*-(trimethylsilyl)benzimidate.[6,13] The mixture was kept for 10 min at room temperature, followed by removal of volatiles under reduced pressure. The product was crystallized by addition of 10 mL of hexane, giving 0.520 g (58% yield) of **1** after decantation of the solution and drying. Mp: 118−120 °C. ^1H NMR ($CDCl_3$, 263 K): δ 2.00, 2.60 (2s, 6H, NMe_2), 5.95 (s, 1H, SiH), 7.20−8.20 (m, 10H, Ph). ^{13}C NMR ($CDCl_3$, 263 K): δ 48.0, 49.6 (NMe_2), 127.6−135.7 (Ph) 163.3 (C=N). ^{29}Si NMR ($CDCl_3$, 300 K): δ −60.9 (d, $^1J_{SiH}$ = 320 Hz). Anal. Calcd for $C_{15}H_{17}ClN_2OSi$: C, 59.1; H, 5.62; N, 9.19. Found: C, 59.42; H, 5.90; N, 9.22.

Bis[*N*-(dimethylamino)pivaloimidato-*N,O*]chlorohydridosilicon(IV) (2b). 2b was prepared as described for **1** from 0.656 g (3.03 mmol) of *N*-(dimethylamino)-*O*-(trimethylsilyl)pivaloimidate[7] and 0.223 g (1.65 mmol) of $HSiCl_3$. After 2 h at room temperature the volatiles were removed and the crystalline residue was separated and dried, to give 0.530 g (99% yield) of **2b**. Mp: 93−94 °C. A single crystal for X-ray diffraction analysis was grown from hexane−CCl_4 solution. ^1H NMR ($CDCl_3$, 300 K): δ 1.09 (s, 18H, t-Bu), 2.85, 2.87 (2s, 12H, NMe_2), 5.13 (s, 1H, SiH). ^{13}C NMR ($CDCl_3$, 300 K): δ 27.0 ($(CH_3)_3C$), 35.0 ($(CH_3)_3C$), 50.0, 50.1 (NMe_2), 174.5 (C=N). ^{29}Si NMR ($CDCl_3$, 300 K): δ −135.9 (d, $^1J_{SiH}$ = 345 Hz). Anal. Calcd for $C_{14}H_{31}ClN_4O_2Si$: C, 47.91; H, 8.90; N, 15.96. Found: C, 47.95; H, 8.86; N, 15.89.

Bis[*N*-(dimethylamino)pivaloimidato-*N,O*]bromohydridosilicon(IV) (2c). A solution of 0.369 g (2.41 mmol) of Me_3SiBr in 10 mL of hexane was added to crude **2b** prepared (see above) from 0.618 g (2.86 mmol) of the pivaloimidate and 0.204 g (1.50 mmol) of $HSiCl_3$. The mixture was kept for 5 min at 60 °C followed by removal of volatiles under vacuum (0.02 mmHg). The residue of colorless crystals of **2c** weighed 0.486 g (86% yield). Mp: 89−90 °C. A single crystal was grown from hexane solution. ^1H NMR (toluene-d_8, 300 K): δ 1.12, 1.15 (2s, 18H, t-Bu), 2.71, 2.78 (2s, 12H, NMe_2), 5.90 (s, 1H, SiH). ^{13}C NMR (toluene-d_8, 190 K): δ 26.7 ($CH_3)_3C$), 35.1, 35.3 ($(CH_3)_3C$), 48.2, 49.7, 50.4, 50.7 (NMe), 173.5, 173.9 (C=N). ^{29}Si NMR (toluene-d_8, 300 K): δ −137.4 (d, $^1J_{SiH}$ = 328 Hz). Anal. Calcd for $C_{14}H_{31}BrN_4O_2Si$: C, 42.53; H, 7.90; N, 14.17. Found: C, 42.89; H, 7.79; N, 14.28.

Bis[*N*-(dimethylamino)acetimidato-*N,O*]hydridosiliconium(IV) Tetrachloroaluminate (5a). 5a was prepared directly in the NMR sample tube from **2a** and excess $AlCl_3$ and characterized by NMR spectral analogy. ^1H NMR (CD_2Cl_2, 300 K): δ 2.12 (s, 6H, Me), 2.90, 2.93 (2s, 12H, NMe_2), 5.26 (s, 1H, SiH). ^{13}C NMR (CD_2Cl_2, 300 K): δ 17.0 (Me), 49.4, 50.3 (NMe), 166.9 (C=N). ^{29}Si NMR (CD_2Cl_2, 300 K): δ −75.3 (d, $^1J_{SiH}$ = 354.7 Hz).

Bis[*N*-(dimethylamino)pivaloimidato-*N,O*]hydridosiliconium(IV) Tetrachloroaluminate (5b). 5b was prepared from **2b** in a manner similar to that for **5a**, directly in the NMR tube. ^1H NMR (CD_2Cl_2, 300 K): δ 1.23 (s, 18H, t-Bu), 2.85, 2.98 (2s, 12H, NMe_2), 5.33 (s, 1H, SiH). ^{13}C NMR (CD_2Cl_2, 300 K): δ 26.8 ($(CH_3)_3C$), 35.9 ($(CH_3)_3C$), 49.0, 50.2 (NMe), 174.6 (C=N). ^{29}Si NMR (CD_2Cl_2, 300 K): δ −75.5 (d, $^1J_{SiH}$ = 357.7 Hz).

Chloro[*N*-(dimethylamino)-(*R,S*)-2-phenylpropionimidato-*N,O*]hydridophenylsilicon(IV) (10). 10 was prepared directly in the NMR sample tube by dissolving equimolar quantities of *N*-(dimethylamino)-*O*-(trimethylsilyl)-(*R,S*)-2-phenylpropionimidate[14] and $PhHSiCl_2$ in $CDCl_3$ (two diastereomers). ^1H NMR (toluene-d_8, 253 K): δ 1.42, 1.43 (2 d, $^3J_{HH}$ = 7 Hz, 3H, CMe), 1.45, 1.47, 1.87, 1.92 (4s, 6H, NMe_2), 3.54, 3.61 (2 q, $^3J_{HH}$ = 7 Hz, 1H, CH), 6.02, 6.04 (2 s, 1H, SiH). ^{13}C NMR ($CDCl_3$, 253 K): δ 17.6, 17.9 (CCH_3), 42.2, 42.3 (CCH_3), 47.8, 48.2, 49.7, 49.8 (NMe), 170.0, 170.2 (C=N). ^{29}Si NMR ($CDCl_3$, 300 K): δ −61.0 (d, $^1J_{SiH}$ = 318.7 Hz), −61.8 (d, $^1J_{SiH}$ = 319.4 Hz).

X-ray Diffraction. Crystal data were collected from a shock-cooled crystal on an Enraf-Nonius CAD4 diffractometer for **1** and on a Bruker SMART CCD 1000 diffractometer for

(13) Kalikhman, I. D.; Bannikova, O. B.; Volkova, L. I.; Gostevskii, B. A.; Yushmanova, T. I.; Lopirev, V. A.; Voronkov, M. G. *Bull. Akad. Nauk SSSR* **1988**, 460; *Chem. Abstr.* **1989**, *110*, 75608c.

(14) Kost, D.; Kalikhman, I.; Krivonos, S.; Stalke, D.; Kottke, T. *J. Am. Chem. Soc.* **1998**, *120*, 4209.

2b,**c**, at low temperatures (see Table 1).[15] The structures were solved by direct methods (SHELXS-97) and refined by full-matrix least-squares methods against F^2 (SHELXL-97).[16] R values are defined as R1 = $\sum||F_o| - |F_c||/\sum|F_o|$ and wR2 = $[\sum w(F_o^2 - F_c^2)^2/\sum w(F_o^2)^2]^{0.5}$, with $w = [\sigma^2(F_o^2) + (g_1P)^2 + g_2P]^{-1}$ and $P = 1/3[\max(F_o^2,0) + 2F_c^2]$. The positions of H(−Si) were taken from the difference Fourier syntheses and refined freely. All other hydrogen atom positions were refined using a riding model. Crystallographic data (excluding structure factors) for the structures reported in this paper have been deposited with the Cambridge Crystallographic Data Centre as Supplementary Publication Nos. CCDC-243085, -243086, and -243087 for compounds **1** and **2b**,**c**, respectively. Copies of the data can be obtained free of charge on application to the CCDC, 12 Union Road, Cambridge CB2 1EZ, U.K. (fax, (internat.) + 44(1223)336-033; e-mail, deposit@ccdc.cam.ac.uk).

(15) Stalke, D. *Chem. Soc. Rev.* **1998**, *27*, 171.
(16) (a) Sheldrick, G. M. *Acta Crystallogr., Sect. A* **1990**, *46*, 467. (b) Sheldrick, G. M. SHELXL-97, Program for Crystal Structure Refinement; University of Göttingen, Göttingen, Germany, 1996.

Acknowledgment. Support from the German Israeli Foundation for Scientific Research and Development (GIF), Grant No. I-628-58.5/1999, and from the INTAS, Project No. 03-51-4164, is gratefully acknowledged. D.S., B.W., T.K., and N.K. appreciate financial support by the Deutsche Forschungsgemeinschaft and the Fonds der Chemischen Industrie.

Supporting Information Available: Tables of crystallographic data for compounds **1** and **2b**,**c**; these data are also available as CIF files. This material is available via the Internet at http://pubs.acs.org.

OM049530K